Flight Test Comparison of Alternate Strategies for Multi-Loop Control Law Optimization

Mohammadreza H. Mansur
mohammadreza.h.mansur.civ@mail.mil

Mark B. Tischler
mark.b.tischler.civ@mail.mil

US Army Aviation Development Directorate – AFDD
Aviation and Missile Research, Development, and Engineering Center
Research, Development, and Engineering Command
Moffett Field, CA, USA

Abstract

The optimization of design parameters in a multi-loop set of control laws against relevant specifications can be carried out using one of two approaches: 1) all design parameters can be simultaneously optimized against all the specifications in a "One-Shot" approach or 2) design parameters for the inner-most loop can be optimized against specifications relevant to that loop only and then the inner-most loop fixed and optimization continued with the next loop in a "Nested" approach. Clearly, the "One-Shot" approach yields the most optimal solution as it allows all specifications to interact with all design parameters within a single optimization process. However, the "One-Shot" approach also results in a much more complex optimization problem that is much more time consuming and prone to optimization pitfalls. The "Nested" approach, on the other hand, results in a simpler optimization problem that is less computationally intensive and less prone to optimization issues, but may not result in achieving the best performance from the system. This paper compares and contrasts the two approaches and outlines an optimization strategy for the "Nested" approach that retains the simplicity and computational benefits of the approach, while yielding results that are comparable to the "One-Shot" results in terms of achieving the best performance from the system. Analysis and flight test results, using U.S. Army AFDD's RASCAL helicopter, are presented and discussed. The flight test results provide design guidance for the velocity and position loop performance not available in the current version of ADS-33.

Symbols

γ^2	Coherence
δ_{BL}	Broken-Loop Sweep Input
δ_{DRB}	Disturbance Sweep Input
e_θ	Mixer Input (pitch)
f_θ	Feedback Response (pitch)
θ	Pitch Attitude
V_x	Longitudinal Ground Speed
ω_{DRB}	Disturbance Rejection Bandwidth

Acronyms

ACAH	Attitude Command Attitude Hold
AFDD	Aeroflightdynamics Directorate
DM	Design Margin
DMO	Design Margin Optimization
DRB	Disturbance Rejection Bandwidth
GM	Gain Margin (dB)
HQR	Handling Qualities Rating
MTE	Mission Task Element
OLOP	Open-Loop Onset Point
PH	Position Hold
PI	Proportional/Integral
PID	Proportional/Integral/Derivative
PIO	Pilot Induced Oscillations
PM	Phase Margin (deg)
RASCAL	Rotorcraft Aircrew Systems Concepts Airborne Laboratory
RCDH	Rate Command Direction Hold
RMS	Root Mean Square
SM	Standard Margins
VH	Velocity Hold

Presented at the American Helicopter Society 69th Annual Forum, Phoenix, Arizona, May 21-23, 2013.

Introduction

Multi-objective parameter optimization of flight control systems has been demonstrated for a number of recent rotorcraft and fixed-wing projects such as in the exploration of trade-offs between stability margins and disturbance rejection bandwidth on the UH-60A [1] and the development of inner-loop control laws for the Kaman unmanned K-MAX [2], cable angle feedback control laws for the RASCAL helicopter [3], pitch axis control laws for the Cessna CJ1 aircraft [4], and control laws for the Tiger Moth UAV [5]. All these projects have used the AFDD-developed Control Designer's Unified Interface (CONDUIT®) software tool [6] to perform the design, analysis, and optimization.

For multi-loop control laws the optimization can be carried out *simultaneously* for all loops (referred to as the "One-Shot" approach) or *one loop at a time* starting from the inner-most loop and building out (referred to as the "Nested" approach) (Figure 1). In the Nested approach, after the inner-most loop is optimized, all gains associated with that loop are fixed before optimization is continued with the next outer-loop, in turn using its associated gains and specifications, and then further out in the same manner. Because with the One-Shot approach all loops are optimized at the same time, the final result will be the most optimal achievable since outer-loop requirements and associated gains can influence inner-loop gains. In contrast, with Nested approach by the time an outer-loop is being optimized all inner-loop gains have been fixed, preventing the outer loop from having any influence on them.

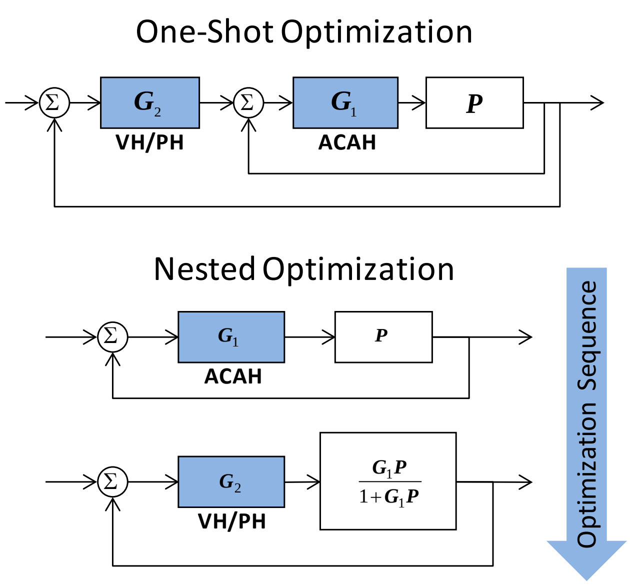

Figure 1 – One-Shot vs Nested optimization approach

On the flip side, the One-Shot approach results in a much larger optimization problem that takes significantly more computational time. In addition, generally speaking the larger the problem size the more likely that the problem will be poorly constrained and the more likely that the optimization engine will get lost or ends up at a local minimum. The Nested approach considers only a part of the entire problem at any given time and therefore is more computationally efficient and the optimization problem tends to be better constrained. An additional advantage of the Nested approach to the designer is significantly increased physical insight owing to the reduced complexity and closer correspondence of the design parameters to the associated requirements.

A central aspect of this research considered the strategy to be followed during Nested approach optimization, and the selection of baseline specifications for the various loops. As mentioned earlier, in the Nested approach the inner-loop is optimized first and then locked while the outer loops are subsequently optimized. The performance of the inner-loop will, therefore, directly affect the performance of the outer-loop because the closed-inner-loop now represents the "effective" bare-airframe being controlled, as shown in Figure 1. A key concern for the Nested approach, therefore, is how to guide the optimization to concurrently achieve both good inner-loop response and the best "effective" bare-airframe characteristics for subsequent outer-loop optimization. The goal is to tailor the Nested approach in a way that ensures overall control system performance comparable to the One-Shot approach.

One possible approach to the optimization of the inner-loop in a Nested design is to use published specifications as fixed requirements. The metrics of importance here are crossover frequencies, stability margins, and disturbance rejection bandwidths (DRB) and disturbance rejection peak-magnitude (DRP). Stability margin requirements are specified in documents such as MIL-F-9490D [7] (now replaced by the SAE AS94900 [8]) while crossover frequency minimums can be determined using preliminary design, as discussed in [6]. Disturbance rejection bandwidth requirements for ACAH response type (only) are specified in the ADS-33 PRF Test Guide [9]. The outer loops can then be built around this optimized inner-loop.

A second possible approach to the optimization of the inner-loop in a Nested design is to maximize performance by increasing the crossover and disturbance rejection boundaries as far as possible while meeting all other requirements. This second approach achieves the tightest inner-loop possible before building the outer-loops around it, at the cost of higher actuator activity. Both methods were looked at as part of this research.

In this paper, competing design approaches are compared in flight for a full authority model-following set of control laws [1] for the UH-60A RASCAL [10] helicopter (Figure 2). These control laws were previously developed and optimized using the One-Shot approach [1] and flight tested. For the research presented here this same set of control laws were optimized using the Nested approach. Both possible approaches to the inner-loop were carried out, resulting in two distinct "Nested" optimization gain sets to compare to the gain set arrived at using the One-Shot approach. The paper compares and contrasts the three gain sets and provides guidance for outer-loop metrics such as velocity DRB.

Figure 2 – The RASCAL JUH-60A variable stability helicopter

Overview of the Model Following Flight Control System (MFCS)

The core of the model-following flight control system (MFCS) for this study is Attitude Command/Attitude Hold (ACAH). The velocity and position hold (VH and PH, respectively) loops are closed around this core in concentric layers, lending itself nicely to the exploration of the Nested optimization approach. Control law response type changes are automatic, with the VH functionality activated with the cyclic stick in detent while the PH functionality is activated when the ground velocity drops below a prescribed threshold. Note that this is different than a Translational Rate Command (TRC) implementation as the pilot never directly commands a translational rate. Speed references are captured automatically when the stick is returned to detent. In the directional axis, the control laws provide a rate command/ direction hold (RCDH) response type, with the hold functionality automatically activated with the pedals in detent. Altitude hold functionality is also provided, but the heave channel uses a simple response feedback architecture instead of model following and the characteristics of the vertical axis response were constant throughout this study. The control laws were only optimized for the hover/low speed regime of flight. The basic feedback architecture for achieving ACAH in pitch and roll and RCDH in yaw is PID. The velocity hold functionality is implemented with an outer loop PI architecture based on the longitudinal and lateral ground velocities. The position hold is, in turn, implemented with an outer-loop proportional architecture based on longitude and latitude. An overview of the system is shown in Figure 3.

Validation of Analysis Model Stability Margins and Predicted Performance

In order to confidently rely on the analysis and safely take the optimized control gains to flight, it's critically important to verify that the analysis model accurately represents the real system. In the case of this study, analyses started with a model that was developed, validated, and documented as part of the trade-off study of 2009 [1]. Nevertheless, standard model validation data was collected early in the flight schedule and the analysis model was revalidated against the current state of the system. The goal was primarily to show that the analysis model correctly predicts the stability margins of the system so that stability-related safety concerns could be addressed prior to flight. Additionally, the ability of the analysis model to accurately predict disturbance rejection bandwidth and closed loop performance was checked. Specialized flight tests were carried out in which automated sweeps were directly injected at the mixer δ_{BL} input and into the sensors δ_{DRB} (Fig. 3) to calculate broken loop and disturbance rejection characteristics of the actual system, respectively. Additionally, closed-loop piloted sweeps were conducted to validate the closed-loop accuracy of the analysis model.

Broken Loop Response

As mentioned above, automated sweeps at the mixer input (Figure 3) were used in flight to generate time responses for each gain set. An example sweep is shown in Figure 4. The pilots were instructed to minimize control inputs as much as possible and limit their inputs to pulse-type corrective inputs, as needed to prevent the aircraft from drifting too far away from trim. Therefore, by default the system would have been in VH mode for these runs as the cyclic stick and pedals were mostly left in detent. In order to evaluate all modes of the control laws (ACAH, VH, PH), however, the desired mode was manually engaged, overriding the default settings, and data were then collected for all modes. Flight test time responses were then processed with the Comprehensive Identification from Frequency Responses (CIFER® [11]) tool to generate broken loop frequency responses for each axis in all modes. These were then compared to frequency responses obtained from the analysis model. Figure 5 shows an example of such a comparison of the broken-loop response for the pitch axis (f_θ / e_θ) with the system in VH mode. As may be seen, for the frequency range of

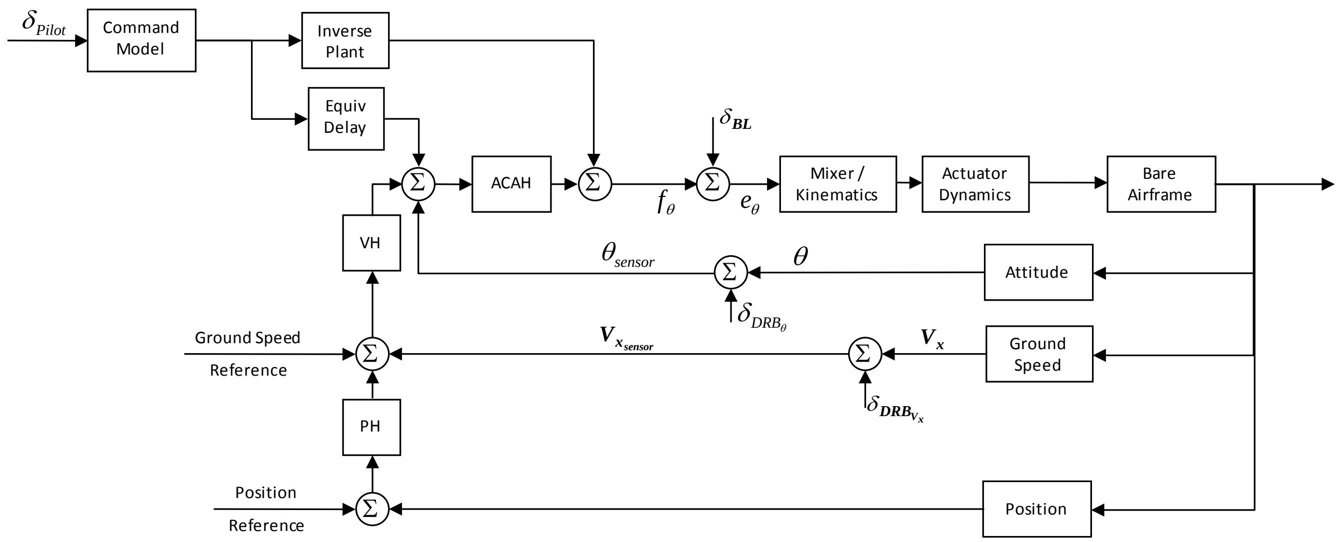

Figure 3 – Overview of control system

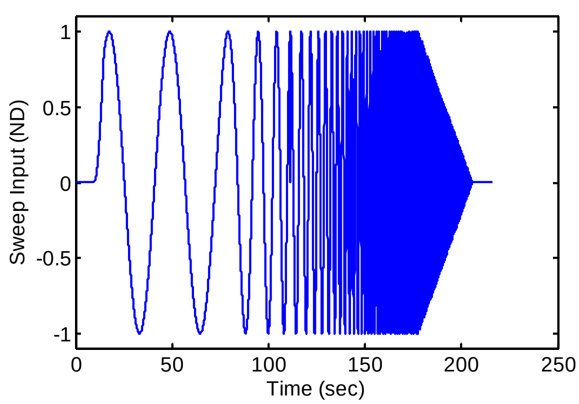

Figure 4 – Example automated sweep input

good coherence $(\gamma^2 > 0.6)$, where the results are reliable, the match between the analysis and flight data is very good. The results indicate that crossover frequency and phase/gain stability margins can be predicted accurately and that the analysis is a good representation of the actual system for margin calculation purposes. Similar accuracy was observed for other axes and modes.

Disturbance Rejection Bandwidth (DRB)

Automated sweeps, this time at the output of the various sensors (Fig. 3), were injected in flight to generate disturbance time responses for each gain set. Note that because the inputs are injected at the sensors, the control system sees the disturbance sweeps as feedback error and responds to it accordingly. Therefore, the aircraft tends to move much more than it does during automated sweeps injected at the mixer. The pilots were instructed to let the system move freely as much as possible and to only use pulse type inputs to prevent the aircraft from drifting too far away from trim. To further ensure good quality data, the maneuver was practiced in the RASCAL Development Facility (DF) to familiarize the pilots with the aircraft response during disturbance sweeps. As before, the automatic mode switching of the system was overridden so that system would be in the appropriate mode for each sweep. Disturbance sweeps were conducted in pitch, roll, and yaw attitudes while the system was in ACAH, and in lateral and longitudinal ground speeds while the system was in VH. Results indicated that the analysis accurately predicted both disturbance rejection bandwidths (DRB) and disturbance rejection peak magnitudes (DRP). Figure 6 compares the analysis model prediction of the heading disturbance response with data obtained from flight and analyzed using CIFER®. As may be seen, the match is quite good and DRB and DRP are predicted well.

Closed Loop Response

Finally, piloted sweeps were performed in each axis (excluding heave) to evaluate the end-to-end response characteristics of the system and collect data for analysis validation. Note that during closed-loop lateral and longitudinal piloted sweeps the cyclic stick is continually out of detent and therefore the system is in ACAH mode. Three 90 second sweeps starting from a minimum frequency of 0.05 Hz (0.3 rps) and ending at a maximum frequency of 2 Hz (12.5 rps) were conducted and the resulting time histories concatenated for CIFER® analysis. Figure 7 presents the comparison of closed-loop, end-to-end, pilot stick (%) to pitch rate response (deg/sec) between analysis and flight. The piloted sweeps were collected under conditions of almost no winds/turbulence resulting in excellent coherence from very low frequencies up to the 2 Hz maximum frequency of the input. Comparison results show that the analysis is a very good representation of the actual aircraft over the same frequency range, providing confidence in the analyses.

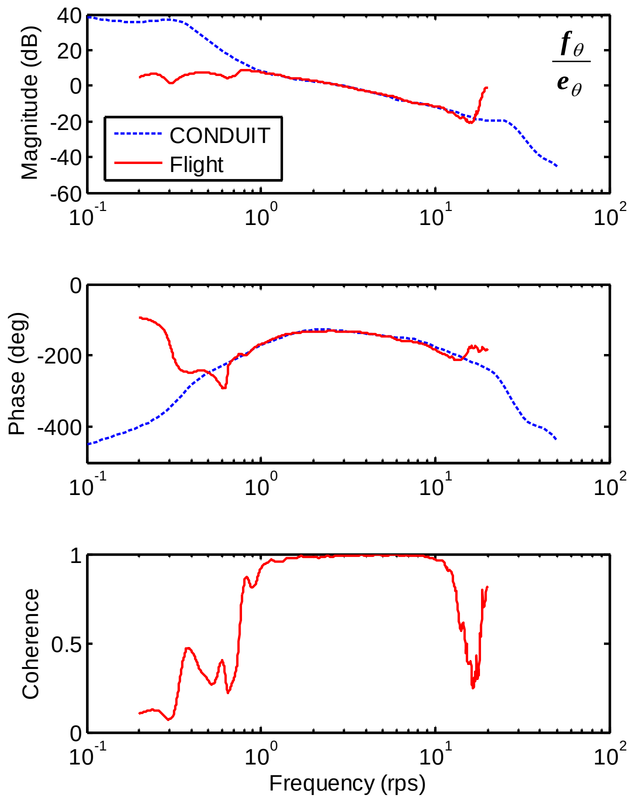

Figure 5 – Analysis validation, broken-loop response, velocity hold mode (f_θ / e_θ)

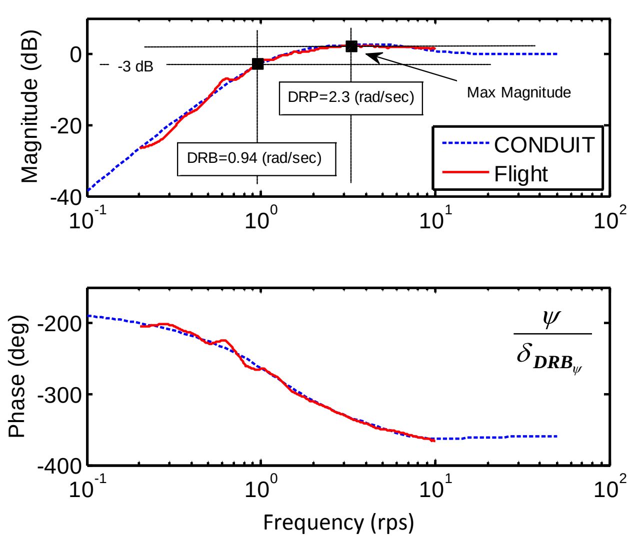

Figure 6 – Analysis validation, disturbance response, (ψ / δ_{DRB_ψ})

Multi-Objective Parameter Optimization

CONDUIT® [6] was used to carry out the control law analyses and optimizations for the effort presented in this paper. The One-Shot approach gain set was taken from the trade-off study of 2009 [1] and corresponded to the configuration with standard stability margins (SM) (phase margin of 45 deg., gain margin of 6 dB). Herein, two sets of gains optimized using the Nested approach were evaluated and compared with the One-Shot results. The first Nested gain set, referred to henceforth as the "ADS-33 Boundaries" gain set, used the previously determined values of minimum crossover frequencies based on preliminary design [6] and published ADS-33 minimum values for attitude DRBs from the ADS-33 Test Guide [9] for the inner-loop (ACAH) specification boundaries. With these inner-loops fixed, the velocity and position loops were then optimized for best achievable velocity DRB and position hold performance. The second Nested gain set, referred to henceforth as the "Extended Boundaries" gain set, first optimized the inner-loop to the highest levels of crossover and attitude DRB achievable before optimizing the velocity and position loops for best achievable velocity DRB and position hold performance.

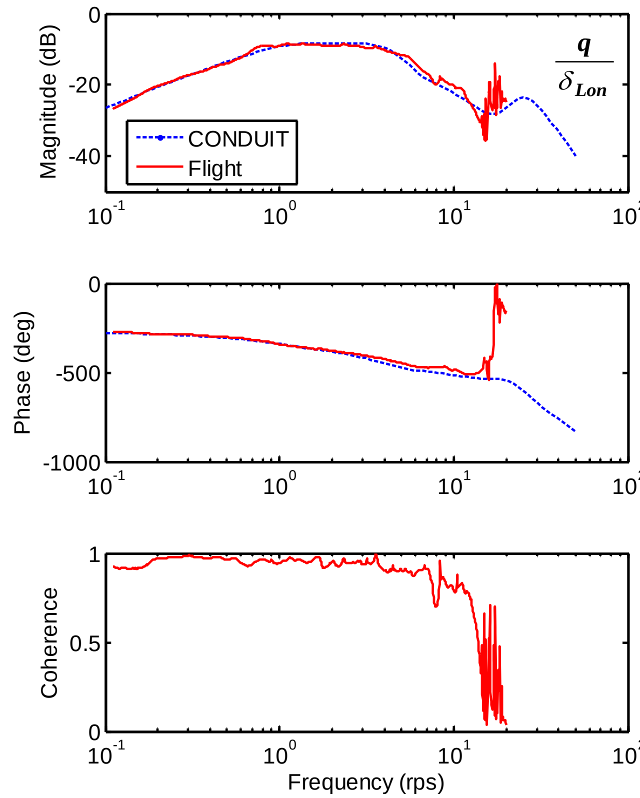

Figure 7 – Analysis validation, closed-loop response, (q / δ_{Lon})

Specifications

The specifications used during this study are listed in Table 1 and encompass requirements for absolute stability, acceptable stability margins, required closed-loop damping, minimum crossover frequency, disturbance rejection bandwidth and peak, Open Loop Onset Point specifications to guard against actuator rate saturation and resulting PIO tendency, and finally actuator RMS and crossover frequency to guard against overdesign. In conjunction, for the inner-loop additional handling qualities requirements such as acceptable pitch to roll coupling and acceptable yaw to heave coupling were enforced. More details about these specifications can be found in references 1-6.

The specifications are divided into 4 categories, as seen in Table 1 and explained in [6]. "Hard constraints" (H-type in Table 1) are specs that relate to the stability of the system and therefore must be satisfied ahead of all others (Phase 1). "Soft constraints" (S-type in Table 1) are specs that relate to handling qualities of the system and are satisfied after all hard constraints are met (Phase 2). When all the stability-related (hard) and handling-qualities-related (soft) constraints are satisfied (at the end of Phase 2) a "feasible", though not yet optimal, control system is reached. Further optimization to ensure satisfaction of all the requirements without overdesign and with minimum achievable gains (cost of feedback) is then carried out (Phase 3) by minimizing a summed objectives function (J-type in Table 1). The final type of specification used is the "check only" type (C-type in Table 1) which cover specifications that are not considered as part of the optimization but whose values are calculated and presented. More detail on the optimization process is given in references 6 and 12.

Design Parameters

In CONDUIT®, the system parameters that are designated as "tuning knobs" in the optimization process are referred to as "Design Parameters" (DPs). Note that not every system parameter is a DP as most systems contain many additional parameters which remain constant throughout the optimization. For the One-Shot approach a total of 15 system parameters consisting of the PID gains in pitch, roll, and yaw, PI gains in longitudinal and lateral velocity, and proportional gains in longitudinal and lateral position, were designated as DPs. Note that of these only 13 DPs were allowed to vary freely during the optimization. The integral gains on longitudinal and lateral ground velocities (Vx and Vy) were constrained to their corresponding velocity gains. This ensures good low-frequency response tracking with minimum stability margin degradation due to the integral function.

In the case of the two Nested approach gain sets, for the inner ACAH loop 6 gains consisting of the proportional angular and rate gains in pitch, roll, and yaw were designated as Design Parameters. The integral gains were tied to the attitude gains such that the ratio of integral to attitude gains equaled 1/5 (1/10 for yaw) of the associated nominal crossover (this will be discussed further later in this paper). In the outer velocity loop again the integral gains were constrained, this time to their associated velocity gains such that the ratio of integral to velocity gains equaled 1/5 of the nominal associated crossover. This left only two of the four PI gains as design parameters. Finally, in the position loop the position gains in longitudinal and lateral axes were design parameters. This results in a total of 10 Design Parameters for the Nested approach.

The product of the number of specifications being evaluated and the number of design parameters can be considered a good representation of the size of the optimization problem. As shown in Table 2, for the One-Shot approach there are 13 design parameters and 76 total specifications leading to a problem size value of 988. For the Nested approach the problem is divided into smaller pieces. The inner-loop has 6 design parameters and 36 specs for a partial size of 216. Then, the outer-loop has a total of 4 design parameters and 40 specs for a partial size of 160. So, the total size for the Nested optimization is the sum of these parts or 376.

This 62% problem size reduction for the Nested approach provides for significant computational efficiency improvement and better physical insight. Therefore, the Nested approach would be preferred if it can be shown to produce results comparable to the One-Shot approach. Keep in mind also that in addition to requiring fewer computations, the smaller size of the problem will make it easier to arrive at a well constrained optimization problem.

Design Margin Optimization (DMO)

In CONDUIT® all specs are divided into 3 regions which roughly correspond to the 3 handling qualities levels of the Cooper Harper rating scale [13], namely Level 1: Acceptable without improvement, Level 2: Deficiencies warrant improvement, and Level 3: Deficiencies require improvement. The goal of the optimization is then to determine Design Parameters that would allow all specifications to be in Level 1 with minimum overdesign. The concept of a Design Margin is based on these levels. A non-zero positive Design Margin in effect moves the boundary between Levels 1 and 2 in the direction of the Level 1 region, increasing the performance at the cost of increasing actuator usage and a tighter design space. The fractional amount by which the Level 1 / Level 2

Table 1 – Design specifications

Name	Description	Type	Comments
EigLoG1	Eigenvalues	H	Ensure stability
StbMgG1	Gain/Phase Margins (rigid-body frequency range)	H	Ensure adequate stability margins (MIL-F-9490D) Margins have to be checked at various points so multiple copies of this spec are used
EigDpG1	Generic Damping Ratio	H	Ensures that all eigenvalues in frequency range of interest have sufficient damping
ModFoG2	Response Comparison (Inner-Loop Only)	S	Ensure responses of aircraft closely match responses of command model
BnwAtH1	Bandwidth (pitch & roll) Other MTEs; UCE>1; Div Att (Inner-Loop Only)	S	Short term pitch/roll response requirement (ADS-33D)
BnwYaH2	Yaw Bandwidth. Other MTEs (Yaw) (Inner-Loop Only)	S	Short term yaw response requirement (ADS-33D)
CrsMnG2	Min. Crossover Freq. (linear scale)	S	Ensure acceptable crossover frequencies
OlpOpG1	Open Loop Operating Point Rate Limit Saturation Spec.	S	Ensure acceptable actuator saturation characteristics and low PIO tendency
DstBwG1	Disturbance Rejection Bandwidth (linear scale)	S	Ensure satisfactory disturbance rejection bandwidth
DstLoG1	Disturbance Rejection Peak Magnitude (Low Freq.)	S	Ensure good damping of disturbance response
RmsAcG1	Position RMS response to CETI turbulence (specialized use of RMS spec)	S	Position Hold Performance
CouYaH1	Coupling Yaw/Collective (Inner-Loop Only)	S	Ensure good yaw/collective coupling (ADS-33D)
RmsAcG1	Actuator RMS	J	Minimizes control overdesign
CrsLnG1	Crossover Freq. (linear scale)	J	Minimizes control overdesign
CouPRH2	Pitch-Roll Coupling Frequency Domain (Inner-Loop Only)	C	Ensure good pitch/roll coupling (ADS-33D)

Table 2 – Reduction in problem size

	Loops	Design Parameters	Specs	Part Size	Size
One-Shot	All	13	76	N/A	988
Nested	ACAH	6	36	216	376 (-62%)
	VH/PH	4	40	160	

boundary is moved into the Level 1 region is equal to the product of the Design Margin and the width of the Level 2 region of the spec. So, for example, a Design Margin of 0.2 means that the Level 1 / Level 2 boundary has moved 20% of the width of the Level 2 region into the Level 1 region. This is depicted in Figure 8. Note that Design Margin can be activated on a per spec basis. Design Margin Optimization was then used to systematically increase crossover frequency, DRB, and other requirements as applicable for the Nested optimization cases (this will be discussed further later in this paper). Design Margin Optimization is a CONDUIT® capability that automates the process of incrementally varying Design Margin values and optimizing the system for these values in a batch process [14]. Note that DMO was also used for the One-Shot case during the 2009 trade-off studies [1].

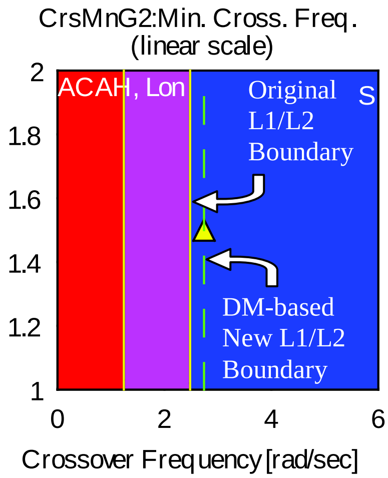

Figure 8 – Effect of Design Margin

Optimization Strategies

One-Shot Optimization Approach

As mentioned earlier, the One-Shot approach gain set was selected from the 2009 stability margin vs disturbance rejection performance trade-off studies and corresponded to the configuration with standard margins.

Nested Optimization Approach

The details of the process used to arrive at the "Extended Boundaries" gain set is given below. Note that the process for the "ADS-33 Boundaries" gain set was exactly the same except the inner-loop simply used the preliminary design and ADS-33 Test Guide boundaries for crossover frequencies and disturbance rejection bandwidths without trying to achieve increased performance.

Inner-loop ACAH is optimized first:

1. The starting values of the crossover frequency boundaries are obtained from preliminary design or prior design experience, as described in [6], namely:
   Pitch: $\omega_{c_\theta} = 2.5\,rad\,/\,sec$,

   Roll: $\omega_{c_\phi} = 2.5\,rad\,/\,sec$,

   Yaw: $\omega_{c_\psi} = 3.5\,rad\,/\,sec$.

   The starting values of the DRB boundaries are those specified in the ADS-33 Test Guide [9], namely:
   Pitch Attitude: $\omega_{DRB_\theta} \geq 0.5\,rad\,/\,sec$,

   Roll Attitude: $\omega_{DRB_\phi} \geq 0.9\,rad\,/\,sec$,

   Yaw Attitude: $\omega_{DRB_\psi} \geq 0.7\,rad\,/\,sec$.
2. In conjunction with the DRB specifications, disturbance rejection peak (DRP) (peak value of the disturbance response function in dB) values are constrained to $DRP \leq 5\,dB$ to ensure good response damping and acceptable response overshoot and oscillations.
3. Attitude integral gains in each axis are tied to the corresponding attitude gain such that the ratio of the integral to attitude gain would be equal to 1/5 of the corresponding crossover frequency, as shown in eq. 1 for the case of roll:.

$$\frac{K_{I_\phi}}{K_\phi} = \frac{\omega_{c_\phi}}{5} \qquad \text{Eq. 1}$$

   This restricts the integral action (and the associated phase lag) to frequencies below 1/5 of crossover and reduces the number of free inner-loop ACAH design parameters (PID gains) to 6 (note again that the heave axis was not being considered for this work). Since the value of crossover changes every time the optimization engine perturbs one of the design parameters, the instantaneous value of crossover calculated using eq. 1 above is too volatile for the optimization process. A less frequently changing value of crossover was therefore desired. Since, as explained earlier, the crossover frequencies are minimized by the optimization engine to guard against overdesign, the crossover frequencies move towards the boundaries of the minimum crossover specifications. Therefore, these boundaries can be used as a good estimates of the actual crossovers. Of course, if these boundaries are moved as part the DMO process, then the augmented value should be used as the crossover frequency estimate and not the starting boundary.
4. With the boundaries in place as discussed, an initial optimization was carried out to find the initial optimized gains. Note that the resulting gains were the gains used as the inner-loop gains for the "ADS-33 Boundaries" gain set. Also, note that if the optimization fails with these boundaries it indicates that the design cannot satisfy ADS-33 requirements and has to be altered before proceeding.
5. Following the initial optimization, DMO is used to systematically increase the required minimum crossovers and attitude DRBs until optimization could not proceed further, indicating that one of the axis has reached its maximum achievable performance.
6. The crossover and DRB specification boundaries for that axis are then moved to 99% of the achieved value and design margin disabled for crossover and DRB in that axis. Note that corresponding design

parameters are not locked so they can vary as needed due to the effects of inter-axis cross coupling.

7. Design margin optimization is then continued, increasing the crossover and DRB boundaries in the remaining axes, until further increases cannot be achieved, again meaning that one of the remaining axes is at its maximum achievable performance. As before, the crossover frequency and DRB boundaries for that axis are then locked at 99% of the achieved values and design margin disabled for those specifications.
8. This process is continued until maximum performance is achieved for all axes, resulting in the tightest design possible.

The inner-loop ACAH design is at this point complete and optimization of the outer loops can begin:

1. All inner-loop specifications are then disabled and all inner-loop design parameters are frozen at their final values. In their place velocity and position hold specifications are enabled and velocity and position hold design parameters freed to vary by the optimization engine.
2. There are no previously published/specified values for velocity and position crossover frequency or DRB. For velocity crossovers nominal minimum values equal to 1/5 of the corresponding attitude crossover are selected. For velocity DRB, nominal initial values (0.15 rad/sec) are selected (increased during DMO) while the DRP boundaries are set at 5dB. For position, crossover frequencies are not tracked and DRBs are constrained to a nominal minimum of 0.1 rad/sec while DRPs are set at 3dB.
3. In the outer velocity loop, as is done in the inner-ACAH loop, the integral gains are tied to their corresponding proportional gains such the ratio of the integral gain to its corresponding proportional gain would equal 1/5 of the corresponding outer-loop crossover.
4. For the velocity loop the metric of primary importance is DRB, while for the position loop the metric of primary importance is the RMS of the position deviations from reference in response to turbulence. In order to be able to use a consistent and repeatable level of turbulence throughout the flight tests, the Control Equivalent Turbulence Inputs (CETI) were used. These control disturbances are the control inputs required to generate aircraft angular and vertical rates in calm conditions that are consistent with rates observed in flight in atmospheric turbulence [15]. Therefore, whereas for the inner ACAH loop crossover frequency and attitude DRB boundaries were increased through DMO to improve system performance, for VH velocity DRB boundaries were systematically increased during DMO while for PH the position RMS boundaries were systematically decreased.
5. An initial outer-loop optimization is then carried out. Note that if this initial optimization fails the boundaries on velocity and/or position crossover frequencies, DRBs, and position RMS can be adjusted to the achieved values and optimization re-tried starting from initial design parameters. Since published specifications were not available any values obtained here can be considered as providing guidance for where the boundaries actually should be.
6. Following the initial outer-loop optimization DMO was used to systematically increase the velocity DRB requirements and lower the allowable position response RMS to CETI turbulence.
7. DMO is continued until further increases in velocity DRB or further decreases in position RMS could not be achieved.

The design is considered final at this point. This process is summarized in Figure 9 and Table 3.

Characteristics of the Final Designs

As described earlier, the Nested optimization approach was used to arrive at two sets of gains with different enforced boundaries for inner-loop crossover frequencies and disturbance rejection bandwidths. Note that the boundaries for these specifications are set at prescribed minimums but the optimization may not result in the actual metric ending up on the boundary and at the prescribed minimum values. This is due to the coupled nature of many specs, all of which must achieve Level 1 during the optimization. Therefore, some metrics may end up at higher values than the prescribed minimums. Consequently, a higher achieved design margin, e.g. 30%, may not indicate a 30% improvement in the metric since the baseline may have optimized to a higher value than the prescribed minimum.

Table 4 compares the inner-loop crossover frequencies and phase and gain stability margins of the three gain sets considered for this research (One-Shot, Nested with ADS-33 boundaries, and Nested with extended boundaries), as calculated from actual flight data using frequency sweep testing methods and CIFER®. Results show that in all axes and for all three gain sets, the phase and gain margins easily satisfy the AS94900 [8] requirements of 45 deg. phase and 6 dB gain margins. Looking at the crossover frequencies, it can be noted that, as designed, the "Extended Boundaries" Nested results are higher than the "ADS-33 Boundaries" values. Note also that the "Extended Boundaries" Nested results have either higher (pitch and yaw) or comparable (roll) crossover frequencies to the One-Shot results.

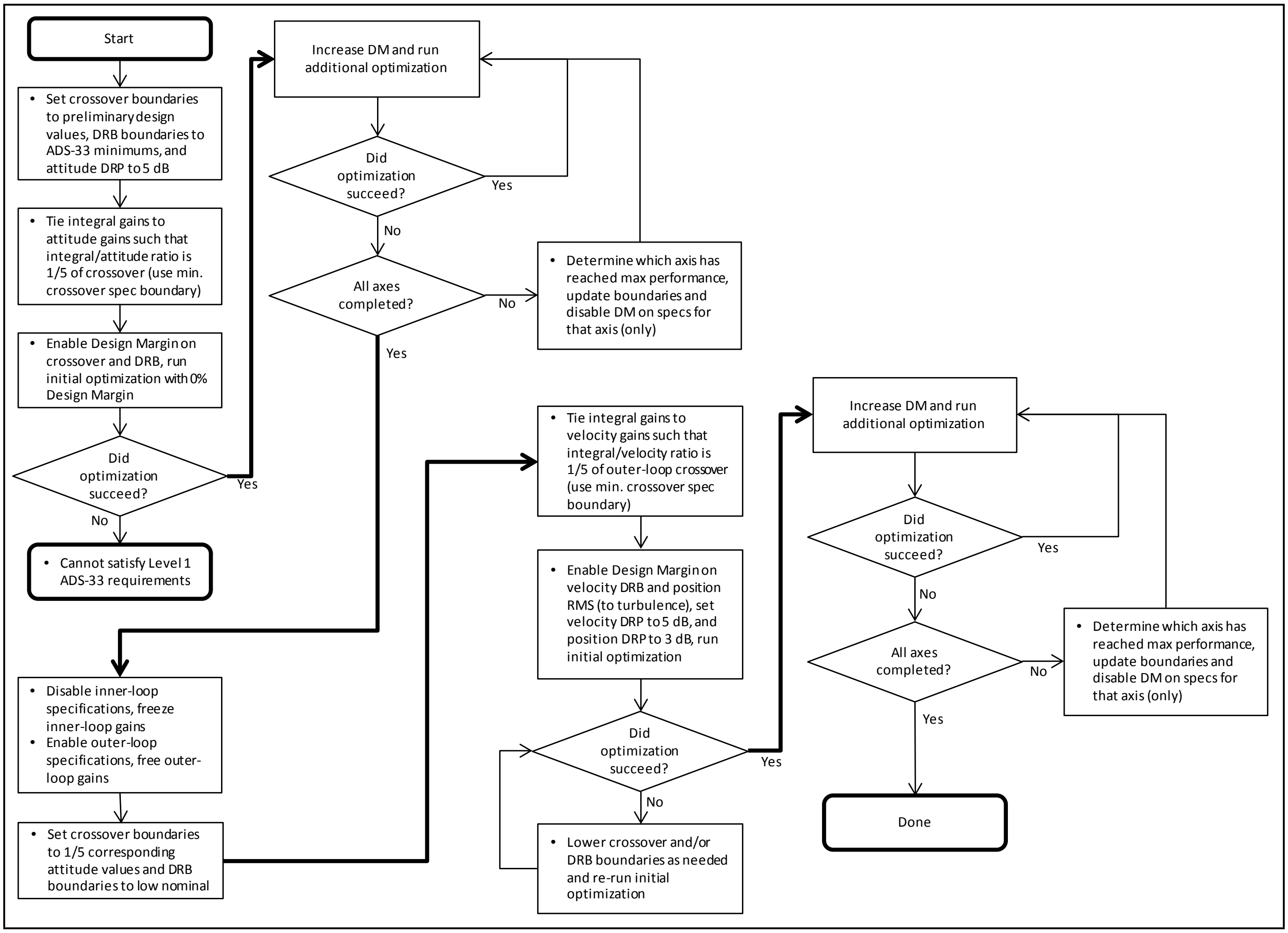

Figure 9 – Graphical representation of Nested optimization approach

Tables 5-6 compare the DRBs and DRPs of the three gain sets as calculated from flight data (disturbance flight data was not collected for PH, therefore analyses results are shown instead). Again, in most cases (except lateral position) the "Extended Boundaries" Nested results achieve higher DRBs than the "ADS-33 Boundaries" results. Note that this is generally accompanied by a higher DRP but the values are much smaller than the allowed maximum of 5 dB.

Results from Tables 4-6 show that the "Extended Boundaries" Nested design has higher crossover frequencies and DRBs than ADS-33 minimums. This will allow the aircraft to hold a reference position better in turbulent conditions and track pilot commands more closely thereby improving predictability. Results also show that the DRB and DRP values for the "Extended Boundaries" Nested gain set are generally comparable to the One-Shot results. This shows that performance comparable to the One-Shot method can be achieved with the simpler/faster Nested approach. Finally, it should be noted that all three designs meet ADS-33 Level 1 Bandwidth requirements for pitch and roll, the minimum values being 3.07 rad/sec and 4.41 rad/sec respectively.

Qualitative and Quantitative Evaluations

Flight tests were carried out to compare the three optimized gain sets discussed above. Two U.S. Army test pilots participated in these flights, carried out at the U.S. Army Aviation Development Directorate - AFDD, Ames Research Center, Moffett Field, California. Qualitative testing for pilot ratings was based on ADS-33 while quantitative testing evaluated ability to achieve and maintain position hold.

Flight Test Maneuvers

Each pilot flew all three gain sets through four ADS-33 hover/low speed MTE's, namely: 1) Precision Hover, 2) Hovering Turn, 3) Lateral Reposition, and 4) Depart/Abort. The flights were flown in as little atmospheric winds and turbulence as possible. Instead,

Table 3 – Tabular representation of Nested optimization approach (*Table courtesy of Tom Berger, UARC, UCSC*)

Baseline Design

Spec	**Attitude Loop (Step 1)**	**VH Loop + (Step 3)**	**PH Loop**
DRB	Minimum values from ADS-33E Test Guide $\omega_{DRB\phi}$ = 0.9 rad/sec $\omega_{DRB\theta}$ = 0.5 rad/sec $\omega_{DRB\psi}$ = 0.7 rad/sec	Set low ($\omega_{u,v} \approx$ 0.15 rad/sec) comes higher due to PH specs	Select value ($\omega_{x,y} \approx$ 0.1-0.2 rad/sec) and set it for optimization and DMO
DRP	≤5 dB	≤5 dB	≤3 dB
Minimum Crossover	Preliminary design	1/5 of attitude loops $\omega_{c\,v} = \omega_{c\,\phi}/5$ $\omega_{c\,u} = \omega_{c\,\theta}/5$	NA
Eigendamping	$\zeta \geq 0.35$, $\omega < \omega_c$ $\zeta \geq 0.2$, $\omega > \omega_c$	$\zeta \geq 0.3$	$\zeta \geq 0.3$
Position RMS to Turbulence	NA	NA	Loose boundaries for initial design
Integral gain	Fixed as ratio of attitude gain: $K_I/K_p = \omega_{c\,\phi,\theta}/5$	Fixed as ratio of velocity gain: $K_I/K_p = \omega_{c\,u,v}/5$	NA
Summed Obj.	Crossover frequency (ω_c), Actuator RMS to attitude disturbances	Crossover frequency (ω_c), Actuator RMS to velocity disturbances	Actuator RMS to position disturbances

Design Margin Optimization

Spec	**Attitude Loop[1] (Step 2)**	**VH Loop + (Step 4)**	**PH Loop**
DRB	Push up	Push up	NA
Minimum Crossover	Push up	NA	NA
Position RMS to Turbulence	NA	NA	Move boundary down to baseline design value, push down from there
Integral gain	Fixed as ratio of attitude gain: $K_I/K_p = \omega_{c\,\phi,\theta}/5$ ω_c taken as boundary of minimum crossover spec	Fixed as ratio of velocity gain: $K_I/K_p = \omega_{c\,u,v}/5$ ω_c fixed thoughout DMO	NA

1. When a particular axis gets stuck: disable DM on that axis; move DRB and Minimum Crossover spec boundaries for that axis to 99% of the last successfully run DM; and continue pushing up on remaining axes. Leave the gains for that axis free. Repeat on stuck axes as necessary.

Table 4 – Flight values for ACAH crossover frequencies and stability margins

	ACAH								
	Pitch			Roll			Yaw		
	Crossover (rad/sec)	Phase Margin (deg)	Gain Margin (dB)	Crossover (rad/sec)	Phase Margin (deg)	Gain Margin (dB)	Crossover (rad/sec)	Phase Margin (deg)	Gain Margin (dB)
One-Shot	2.57	54.1	13.6	4.32	59.0	6.9	4.34	51.3	7.1
ADS-33 Boundaries	2.47	52.7	12.0	2.94	62.3	9.6	4.03	62.8	8.4
Extended Boundaries	2.96	50.2	10.4	4.05	62.6	7.2	4.72	56.6	No Data

Table 5 – Flight values for ACAH disturbance rejection bandwidth (DRB) and disturbance rejection peak (DRP)

	DRB Theta (rad/sec)	DRP Theta (dB)	DRB Phi (rad/sec)	DRP Phi (dB)	DRB Psi (rad/sec)	DRP Psi (dB)
One-Shot	0.60	2.96	1.08	3.86	1.19	3.50
ADS-33 Boundaries	0.46	3.20	1.03	4.21	0.74	1.75
Extended Boundaries	0.63	3.14	1.10	4.28	0.94	2.31

Table 6 – Flight/Analysis values for VH/PH DRB and DRP

	Flight				Analysis *(Flight Data Not Collected)*			
	DRB Vx (rad/sec)	DRP Vx (dB)	DRB Vy (rad/sec)	DRP Vy (dB)	DRB X (rad/sec)	DRP X (dB)	DRB Y (rad/sec)	DRP Y (dB)
One-Shot	0.43	4.38	0.83	2.78	0.17	2.62	0.17	1.65
ADS-33 Boundaries	0.34	3.83	0.54	1.45	0.13	3.00	0.22	2.74
Extended Boundaries	0.40	4.67	0.71	1.63	0.17	2.56	0.17	1.77

CETI synthetic turbulence [15] was used to evaluate the effect of turbulence using a quantifiable and repeatable level of turbulence. The Precision Hover and the Hovering Turn MTEs were flown both with and without CETI turbulence.

In addition, Decel to Position Hold maneuvers were performed to accurately quantify and compare the velocity and position hold performances of the three gain sets in the presence of moderate turbulence. The control laws were designed such that if the pilot returns the cyclic stick to detent with a ground speed less than 5 kts, a deceleration mode is initiated which slows the aircraft down towards hover until ground speed falls below 0.5 kts at which point position hold functionality is engaged. The Decel to Position Hold maneuver was designed to measure the time between the return of the cyclic stick to detent and engagement of position hold mode. The pilots were asked to then leave the stick in detent and the system in position hold for 60 seconds. Here the position hold performance in the presence of CETI turbulence was used to compare the performance of the three gain sets. Finally, the pilots were asked to comment about the perceived speed of response, precision, and ride quality.

In order to better differentiate between the gain sets and gather more information about pilot's perceptions each gain set, a specialized questionnaire that included the traditional Cooper-Harper Handling Qualities Ratings [13] was used after each MTE. As seen in Figure 10, the pilots were asked to rate their ability to perform each of the MTE's with each of the gain sets in 5 categories, namely: 1) ability to be aggressive, 2) level of precision that could be obtained, 3) ride quality during the maneuver, 4) predictability of the aircraft response to pilot inputs, and finally 5) overall handling qualities using the traditional Cooper-Harper Handling Qualities Rating Scale. In addition, the pilots were asked about which sub-phase of the MTE they felt was the major determining factor in the overall Handling Quality Rating (HQR) and also to make comments about anything else that may have influenced their evaluation. The Aggressiveness Rating

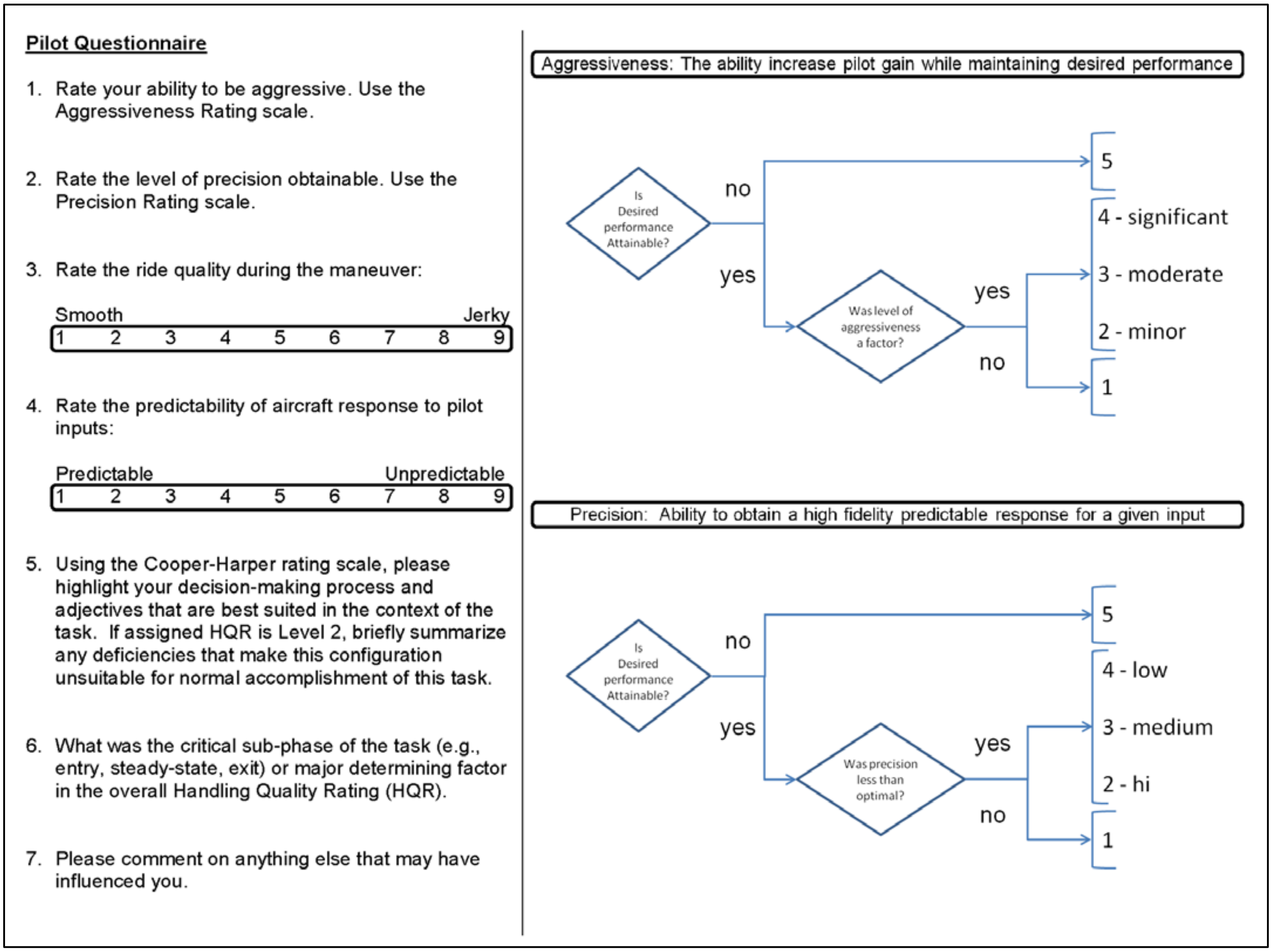

Figure 10 – Pilot questionnaire

scale, the Precision Rating scale, and the other components of the questionnaire used here were developed by Lusardi, et. al. [16].

The three gain sets were flown back-to-back for each MTE. The One-Shot gain set was always flown first because that gain set was from a previous study and somewhat familiar to the pilots. One of the two Nested gain sets was flown next, at random, followed by the remaining Nested set. The pilots were not given any information about the Nested gain set being flown and the order was changed between MTEs ("blind evaluation"). In some cases the One-Shot gain set was re-flown at the end and re-rated to determine the effect of practice on the ratings. In every case the new ratings were almost exactly the same as the original ratings.

Flight Test Results

Results for the four MTEs flown are presented in Tables 7-12. The tables cover all ratings for all the elements of the questionnaire discussed above for all three gain sets. Only the average of the ratings given by the two pilots, including any repeat runs as applicable, are provided.

Tables 7 and 8 present the results for the Precision Hover maneuver, without and with turbulence respectively. As may be seen, for the case without turbulence (Table 7) all three gain sets are rated Level 1 (HQR < 3.5) with the "ADS-33 Boundaries" Nested and the One-Shot gain sets being rated slightly better than the "Extended Boundaries" gain set. These results validate the proposed DRB boundaries for ACAH [9] and suggest boundaries for VH and PH. In contrast, for the case with turbulence (Table 8) the "Extended Boundaries" Nested gain set is rated better than the "ADS-33 Boundaries" gain set, as would be expected based on its higher crossover frequencies and DRBs in all axes (except lateral PH) (Tables 4-6). In fact, the "ADS-33 Boundaries" gain set drops to Level 2 (HQR = 4). Surprisingly, for the case without turbulence, the ratings for aggressiveness, precision, ride quality, and predictability are not consistent with the HQR ratings since the "Extended boundaries" Nested gain set is rated better than the "ADS-33 Boundaries" gain set for all four categories.

Tables 9 and 10 present the results for the Hover Turn maneuver, without and with turbulence respectively. As may be seen, the "Extended Boundaries" Nested gain set is rated better than the "ADS-33 Boundaries" gain set. Nevertheless, for the Hover Turn MTE the "ADS-33 Boundaries" gain set provides Level 1 handling qualities even in the presence of turbulence, again validating the ADS-33 Test Guide [9] recommendations for DRB. Note also that the ratings for aggressiveness, precision, ride quality, and predictability support the HQR results. Finally, note that the results for "Extended Boundaries" Nested are again comparable to the One-Shot results, confirming that the Nested approach can produce designs comparable to the One-Shot approach in terms of handling qualities and performance.

It should be mentioned that this was the first time that CETI turbulence was used to fly ADS-33 MTE's. Pilot comments indicated that the "feel" of the turbulence was realistic and that it introduced an appropriate increase in difficulty in performing the task. Results indicate that it provided a useful means of highlighting differences in performance between the gain sets.

Table 11 presents the results for the Depart/Abort maneuver. The Depart/Abort MTE is not strictly a hover/low speed maneuver but the dynamic portions of the MTE encompass low speed and transition from and to hover. In the presence of winds, this maneuver is usually flown both upwind and downwind so that the pilot can comment on any noticeable differences in flight characteristics. For the present study both pilots flew this MTE in conditions of clam winds and did not note any differences based on direction of flight.

As Table 11 indicates, again the "Extended Boundaries" Nested gain set garnered slightly better HQR ratings than the "ADS-33 Boundaries" and the One-Shot gain sets, though all three gain sets were rated Level 1. Again, the aggressiveness, precision, ride quality, and predictability ratings support the HQRs. Note, however, that the maneuver completion times between the three gain sets were virtually identical.

Table 12 presents the results for the Lateral Reposition maneuver. Like the Depart/Abort MTE, the Lateral Reposition is also not strictly a hover/low speed maneuver but the dynamic portions of the MTE encompass low speed and transition from and to hover. Also like the Depart/Abort MTE, the Lateral Reposition maneuver is flown both upwind and downwind in the presence of winds but for this study both pilots flew the maneuver in calm winds and could not note a significant difference that would affect ratings.

As Table 12 shows, again the "Extended Boundaries" Nested gain set is rated better than the "ADS-33 Boundaries" gain set, though both gain sets were rated Level 1. The aggressiveness, precision, ride quality, and predictability ratings support the HQR ratings but note that surprisingly, the maneuver completion time for the "ADS-33 Boundaries" Nested gain set is actually shorter than that of the "Extended Boundaries" gain set.

Table 13 and Figure 11 present results for the decel to position hold maneuver. The decel portion was entered from three different starting states: 1) longitudinal only translation, 2) lateral only translation, and 3) translation in both longitudinal and lateral directions. This was done to ensure that the results would not be starting point specific. As mentioned before, the pilot was asked to fly the aircraft to just above the decel mode threshold (5 kts ground speed) and then nudge the aircraft back under the threshold and immediately put the cyclic back in detent. The time between the engagement of the decel mode and the engagement of position hold was measured. The shorter this time, the tighter the velocity hold loop. Of course, at some point shorter times would indicate that the response is too aggressive to be desirable. Therefore, the pilots were asked to provide comments about the precision and the ride quality of the decel phase of the maneuver.

As Table 13 indicates, the decel times for the "Extended Boundaries" Nested gain set were on average about half that of the "ADS-33 Boundaries" gain set. This indicates a much tighter velocity hold loop. Note that this result is supported by the increase in longitudinal and lateral velocity DRB from the "ADS-33 Boundaries" gain set to the "Extended Boundaries" gain set noted in Table 6. However, the numbers is Table 5 perhaps don't indicate a factor of 2 difference between the two gain sets. It should be mentioned that the pilot comments regarding the ride quality did indicate a slight degradation in ride quality for the "Extended Boundaries" gain set compared to the "ADS-33 Boundaries" gain set, though the degradation was very small and both gain sets were considered to have good ride quality. Note also that the average decel times for the "Extended Boundaries" Nested gain set is slightly better than those for the One-Shot gain set, even though Table 6 shows both longitudinal and lateral velocity DRBs for the One-Shot gain set to be higher than the

Table 7 – Precision Hover, CETI Off (lower is better for all values)

	CETI	Avg. Time (sec)	Aggressiveness	Precision	Ride Quality	Predictability	HQR
One-Shot	Off	4.22	1.67	1.33	2.33	2.33	2.33
ADS-33 Boundaries	Off	4.56	2	2.33	3	2.5	2.33
Extended Boundaries	Off	4.62	1.67	2.17	2.67	1.83	2.5

Table 8 – Precision Hover, CETI On (lower is better for all values)

	CETI	Avg. Time (sec)	Aggressiveness	Precision	Ride Quality	Predictability	HQR
One-Shot	On	4.45	2.25	2.5	3.75	3	3
ADS-33 Boundaries	On	4.25	3.25	3.5	4.50	3.75	4
Extended Boundaries	On	4.00	2.25	2.25	4.25	2.75	2.5

Table 9 – Hovering Turn, CETI Off (lower is better for all values)

	CETI	Avg. Time (sec)	Aggressiveness	Precision	Ride Quality	Predictability	HQR
One-Shot	Off	12.27	1	1.5	2	2	2
ADS-33 Boundaries	Off	11.72	2	1.5	2	3	2
Extended Boundaries	Off	11.25	1	1	2	1.5	1.5

Table 10 – Hovering Turn, CETI On (lower is better for all values)

	CETI	Avg. Time (sec)	Aggressiveness	Precision	Ride Quality	Predictability	HQR
One-Shot	On	11.26	2	2	3.5	2.5	2.5
ADS-33 Boundaries	On	11.58	3	3.5	4.5	4.25	3
Extended Boundaries	On	11.48	1.5	1.5	4	2.5	2

Table 11 – Depart/Abort, CETI Off (lower is better for all values)

	CETI	Avg. Time (sec)	Aggressiveness	Precision	Ride Quality	Predictability	HQR
One-Shot	Off	24.28	2.5	2.5	2	2.75	3
ADS-33 Boundaries	Off	23.85	2.5	3	2	2.75	3
Extended Boundaries	Off	23.94	2.25	2.25	2	2.25	2.75

Table 12 – Lateral Reposition, CETI Off (lower is better for all values)

	CETI	Avg. Time (sec)	Aggressiveness	Precision	Ride Quality	Predictability	HQR
One-Shot	Off	17.21	2.25	2.5	2	2.5	3.25
ADS-33 Boundaries	Off	16.88	2.5	3	2	3.25	3
Extended Boundaries	Off	17.40	2	2	2	2.5	2.88

Table 13 – Decel to PH times

Direction	One-Shot (sec)	ADS-33 Bounds (sec)	Extended Bounds (sec)
Forward	5.9	8.8	6.0
Right	5.8	10.6	5.8
Quartering	6.1	12.2	5.1
Average	5.93	10.53	5.63

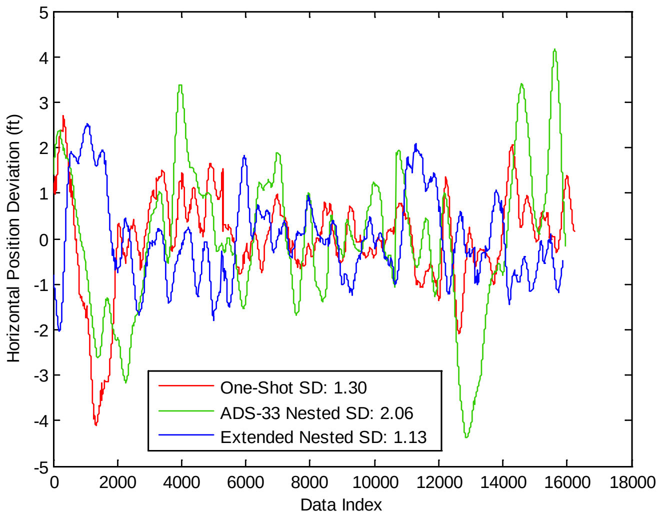

Figure 11 – Position standard deviation in PH

corresponding values for the "Extended Boundaries" Nested gain set.

Finally, Figure 11 depicts the position deviation from reference during the 60 second segments after entering position hold during the decel to position hold maneuvers. For each gain set three 60 second segments, corresponding to the data presented in Table 13, are shown. The legend in Figure 11 indicates the standard deviation of the position error for each gain set. As may be seen, the position deviation for the "Extended Boundaries" gain set is about half that of the "ADS-33 Boundaries" gain set, indicating improved position hold capability. The "Extended Boundaries" results are seen to again be even better than the One-Shot results.

Discussion

Overall, flight test results show that the pilots preferred the "Extended Boundaries" Nested approach gain set to the "ADS-33 Boundaries" gain set. This indicates that when optimizing a multi-mode set of control laws using the Nested optimization approach, better results can be achieved if the inner-loop performance is increased beyond the minimums required by preliminary design considerations and by the currently stated requirements for DRB in ACAH [9] and the minimum values for VH and PH from Table 6. Nevertheless, flight test results also indicate that the currently specified requirements do indeed result in a Level 1 aircraft, at least for calm winds and turbulence. In the presence of moderate or higher winds and turbulence, however, the design may degrade into Level 2.

Finally, flight test results showed that for most maneuvers, the pilots found the "Extended Boundaries" Nested gain set to be comparable to, if not slightly better than, the One-Shot gain set. This shows that it is indeed possible to achieve results comparable to the One-Shot approach using the much simpler and faster Nested approach, if the proper strategy (Figure 8 / Table 3) is followed during the optimization process.

Conclusions

Analysis and optimizations were carried out to compare two strategies for multi-objective parameter optimization of multi-loop flight control laws. Gain sets obtained using the two approaches were flight tested and handling qualities ratings were collected for various hover/low-speed ADS-33 MTEs, some in the presence of CETI turbulence. Results indicated that:

1. The Nested optimization approach can be used along with current specifications to achieve Level 1 handling qualities for calm winds and turbulence.
2. In order to achieve Level 1 handling qualities in the presence of winds and turbulence extended requirements on crossover frequency and disturbance rejection bandwidth may be needed.
3. The Nested approach can produce results that are comparable to those obtained using the One-Shot approach if an appropriate optimization strategy is employed.
4. CETI turbulence can be used in conjunction with ADS-33 MTE's as an effective tool to evaluate handling qualities in the presence of controllable and repeatable turbulence.

Acknowledgements

The authors would like to convey their gratitude to the RASCAL team consisting of Mr. Kevin Kalinowski, Mr. Dennis Zolo, Mr. Ernie Moralez, and Mr. Jay Fletcher. The authors would also like to thank the test pilots, LTC Carl Ott and LTC Mike Olmstead.

References

[1] Mansur, M. H., Lusardi, J. A., Tischler, M. B., and Berger, T., "Achieving the Best Compromise between Stability Margins and Disturbance Rejection Performance," presented at the American Helicopter Society 65th Annual Forum, Grapevine, TX, May 2009.

[2] Mansur, M. H., Tischler, M. B., Bielefield, M. D., Bacon, J. W., Cheung, K. K., Berrios, M. G., and Rothman, K. E., "Full Flight Envelope Inner-Loop Control Law Development for the Unmanned K-MAX®," presented at the American Helicopter Society 67th Annual Forum, Virginia Beach, VA, 2011.

[3] Ivler, C. M., Powell, J. D., Tischler, M. B., Fletcher, J. W., and Ott, C., "Design and Flight Test of a Cable Angle/Rate Feedback Flight Control System for the RASCAL JUH-60 Helicopter," presented at the American Helicopter Society 68th Annual Forum, Fort Worth, TX, May 1-3, 2012.

[4] Berger, T., Tischler, M. B., Hagerott, S. G., Gangsaas, D., and Saeed, N., "Longitudinal Control Law Design and Handling Qualities Optimization for a Business Jet Flight Control System," presented at the AIAA Atmospheric Flight Mechanics Conference, Minneapolis, MN, August 2012.

[5] Fujizawa, B. T., Tischler, M. B., Arlton, P. E., Arlton, D. J., "Control System Development and Flight Testing of the Tiger Moth UAV," presented at the American Helicopter Society 68th Annual Forum, Fort Worth, TX, May 1-3, 2012.

[6] Tischler, M. B., Ivler, C. M., Mansur, M. H., Cheung, K. K., Berger, T., Berrios, M., "Handling Qualities Optimization and Trade-offs in Rotorcraft Flight Control Design," presented at AHS Specialists Meeting on Rotorcraft Handling-Qualities, Liverpool, U.K., November 4-6, 2008.

[7] Anon., "Flight Control Systems - Design, Installation, and Test of Piloted Aircraft, General Specification for," U.S. Air Force, MIL-F-9490D, 6 June 1975.

[8] Anon., "Aerospace - Flight Control Systems - Design, Installation and Test of Piloted Military Aircraft, General Specification for," SAE Aerospace Standard, AS94900, July 2007.

[9] Blanken, C.L., Hoh, R.H., Mitchell, D.G., and Key, D.L, "Test Guide for ADS-33E-PRF," U.S. Army RDECOM special report AMR-AF-08-07, July 2008.

[10] Fletcher, et. al., "UH -60M Upgrade Fly-By-Wire Flight Control Risk Reduction using the RASCAL JUH-60A In-Flight Simulator," presented at American Helicopter Society 64th Annual Forum, Montreal, Canada, April 29 - May 1, 2008.

[11] Tischler, M. B., Remple, R. K., "Aircraft and Rotorcraft System Identification: Engineering Methods and Flight Test Examples, Second Edition," AIAA, October 2012.

[12] Tischler, M. B., Colbourne, J. D., Morel, M. R., Biezad, D. J., Cheung, K. K., Levine, W. S., Veronica, M., "A Multidisciplinary Flight Control Development Environment and Its Application to a Helicopter," IEEE Control System Magazine, Vol. 19, No. 4, pp 22-33, August 1999.

[13] Cooper, G. E., Harper, R. P., "The Use of Pilot Rating in the Evaluation of Aircraft Handing Qualities," NASA TN D-5153, April 1969.

[14] Anon, "CONDUIT User's Guide, Version 6.1.00," University Affiliated Research Center, Moffett Field, CA.

[15] Lusardi, J. A., von Gruenhagen, W., Seher-Weiss, S., "Parametric Turbulence Modeling for Rotorcraft Applications, Approach, Flight Tests and Verification," presented at the Rotorcraft Handling Qualities Conference, University of Liverpool, UK, Nov 2008.

[16] Lusardi, J. A., Blanken, C. L., Ott, C. R., Malpica, C. A., and von Gruenhagen, W., "In Flight Evaluation of Active Inceptor Force-Feel Characteristics and Handling Qualities," presented at the American Helicopter Society 68th Annual Forum, Fort Worth, TX, May 1-3, 2012.